

A CIRCUMSTELLAR DISK IN A HIGH-MASS STAR-FORMING REGION

MICHELE R. PESTALOZZI,¹ MOSHE ELITZUR,² JOHN E. CONWAY,¹ AND ROY S. BOOTH¹

Received 2003 December 18; accepted 2004 January 22; published 2004 February 17

ABSTRACT

We present an edge-on Keplerian disk model to explain the main component of the 12.2 and 6.7 GHz methanol maser emission detected toward NGC 7538 IRS 1N. The brightness distribution and spectrum of the line of bright masers are successfully modeled with high amplification of background radio continuum emission along velocity-coherent paths through a maser disk. The bend seen in the position-velocity diagram is a characteristic signature of differentially rotating disks. For a central mass of $30 M_{\odot}$, suggested by other observations, our model fixes the masing disk to have inner and outer radii of ~ 350 and ~ 1000 AU.

Subject headings: accretion, accretion disks — ISM: kinematics and dynamics — masers — stars: formation — stars: individual (NGC 7538 IRS 1N)

On-line material: color figures

1. INTRODUCTION

Disks are expected to form during protostellar collapse, and low-mass stars seem to provide good observational evidence for the existence of disks (e.g., Qi et al. 2003; Fuente et al. 2003). The situation is less clear for high-mass stars. While in several cases velocity gradients in massive star-forming regions have been detected on large scales ($>10,000$ AU; e.g., Sandel, Wright, & Forster 2003), evidence for compact disks on scales ≤ 1000 AU remains sparse. One possible example is IRAS 20126+4104, where there is good evidence for disk-outflow geometry around a $24 M_{\odot}$ central object (Cesaroni et al. 1999; Molinari et al. 2000). The case for a disk around G 192.16–3.82, a protostar of $\sim 15 M_{\odot}$ (Shepherd et al. 2001), is less compelling.

Class II methanol maser emission, a signpost of high-mass star formation (Minier, Conway, & Booth 2001), offers a potential indicator of disks since it often shows linear structures in both space and position—line-of-sight (LOS) velocity diagrams (Norris et al. 1998; Minier et al. 2000). These masers have been modeled as occurring at fixed radii within edge-on disks, although it is still unclear whether they arise primarily in disks or outflows (DeBuizer 2003; Moscadelli et al. 2002). One of the most striking examples of a maser line in both space and velocity is found in NGC 7538 IRS 1N (Minier et al. 1998, 2000). We present here the first quantitative Keplerian disk analysis of this maser without invoking the assumption of a single radius. We find compelling evidence for the disk interpretation in this case.

2. MASER DATA AND OTHER OBSERVATIONS

The NGC 7538 IRS 1 star formation region has been extensively studied at several wavelengths. The spectral type of the central star has been estimated as O6 (Willner 1976; Campbell & Thompson 1984), in agreement with the spectral energy distribution from 2 mm (Akabane, Matsuo, & Kuno 2001) to $850 \mu\text{m}$ (Momose et al. 2001), which implies a central object with luminosity of greater than $8.3 \times 10^4 L_{\odot}$ and mass of about $30 M_{\odot}$. Very Large Array observations uncovered an associated ultracompact H II region with peak brightness temperature

10,000–15,000 K (Campbell 1984; Gaume et al. 1995). Radio free-free continuum and recombination line observations show a north-south elongated structure attributed to a large-scale outflow.

The first VLBI observations of the 12.2 GHz methanol masers (Minier et al. 1998, 2000) revealed several groups of spots corresponding to different features in the single dish spectra. The subject of our study is the maser in the main spectral feature between about -56.50 and -56.82 km s^{-1} . The 12.2 GHz data cube from published data by Minier et al. (2001), made from 1998 Very Long Baseline Array (VLBA)³ observations, is shown in Figure 1. The interpretation of the linear structure in space and velocity as an edge-on disk (Minier et al. 1998) is supported by the positional agreement of the maser line with the waist of the hourglass-shaped continuum radio emission (Gaume et al. 1995) and a band of free-free absorption. The same structure is evident in the 6.7 GHz maser data, obtained in 2001 February with the European VLBI Network (EVN),⁴ shown in the figure. Taking into account the different angular resolution, the velocity-integrated emission of the two masers is similar out to ± 20 mas in R.A. (Fig. 1, *left*). In addition, the 6.7 GHz data show two disconnected “outlier” maser features that lie close to the extrapolation of the maser line. The right panels in Figure 1 show the position-velocity diagrams for the two masers. They both show the same velocity gradient near the center and a bend at ~ 15 mas.

The 12.2 GHz line involves the $2_0 \rightarrow 3_{-1} E$ transition and the 6.7 GHz line the $5_1 \rightarrow 6_0 A^+$ transition. Since *E*- and *A*-methanol can be regarded as distinct molecules for all practical purposes, the two masers can be expected to probe different physical conditions even when they reside in the same region. Yet in spite of these differences, the brightness peaks of the two lines are perfectly coincident in both velocity and spatial location. The agreement is within the 12.2 GHz angular resolution of 2–3 mas and the spectral resolutions of 0.048 and 0.09 km s^{-1} per channel for the 12.2 and 6.7 GHz data, respectively. Convolution of the 12.2 GHz data to the 6.7 GHz spatial resolution, we find that the ratio of the two emissions is constant to within 10% over the entire feature.

¹ Onsala Space Observatory, SE-43992 Onsala, Sweden; michele@oso.chalmers.se, jconway@oso.chalmers.se, roy@oso.chalmers.se.

² Department of Physics and Astronomy, University of Kentucky, 177 Chemistry/Physics Building, Lexington, KY 40506-0055; moshe@uky.edu.

³ The VLBA is operated from the National Radio Astronomy Observatory’s Array Operation Center in Socorro, NM.

⁴ The EVN is a joint facility of European, Chinese, South African, and other radio astronomy institutes.

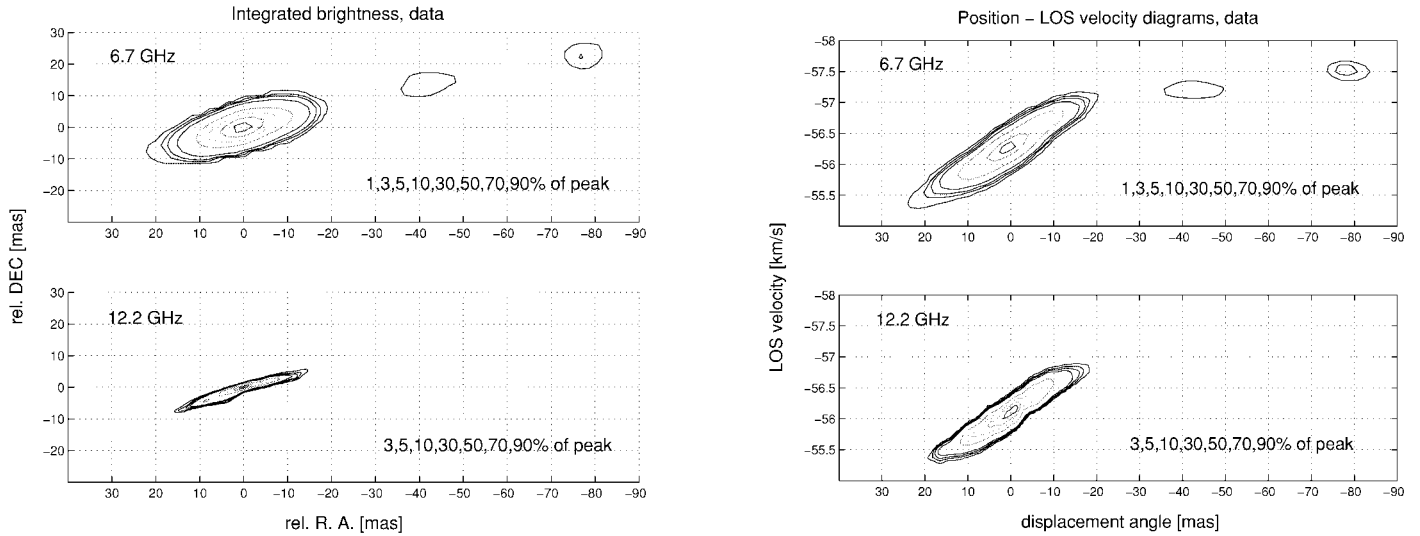


FIG. 1.—*Left*: Zero moment (integrated emission over velocity) maps of the 6.7 and 12.2 GHz methanol masers in the main spectral feature of NGC 7538 IRS 1N. *Right*: (θ, v) -diagrams of the two masers, in which the data have been averaged over the spatial direction perpendicular to the major axis position angle. [See the electronic edition of the *Journal* for a color version of this figure.]

3. MODELING

The remarkable coincidence in space and frequency of the two masers is in fact a natural consequence of amplification of a background source by an edge-on rotating disk. In that case the maser brightness at displacements θ and v from the position and velocity of the LOS diameter is $I(\theta, v) = I_B e^{\tau(\theta, v)}$, where I_B is the background continuum and $\tau(\theta, v)$ the maser (negative) optical depth. Irrespective of the disk annuli where the masers reside, the peak emission will always occur at $(\theta, v) = (0, 0)$, which picks out the largest optical depth τ_0 . With brightness temperature of 10^4 K for the background continuum, the function $\tau(\theta, v) = \ln [I(\theta, v)/I_B]$ is a measured quantity. We find $\tau_0 = 18.32$ and 15.99 for the 6.7 and 12.2 GHz masers, respectively.

Consider an edge-on rotating disk at distance D and a point

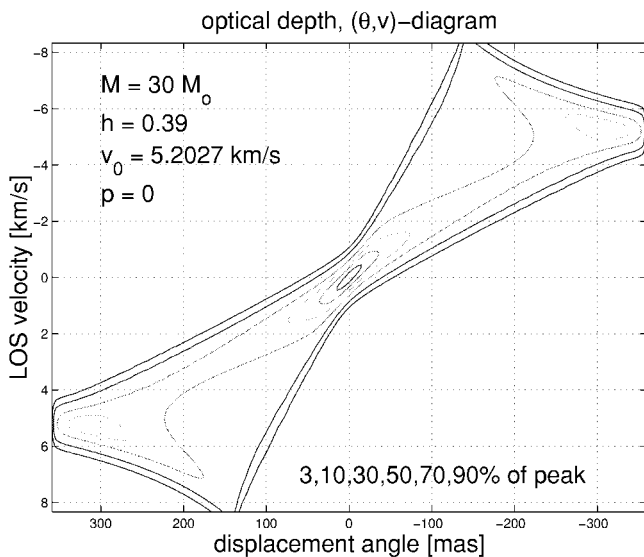


FIG. 2.—Contour plots of $\tau(\theta, v)$ (see eq. [1]) for a Keplerian disk with $\Delta v_D = 0.40 \text{ km s}^{-1}$ around a $30 M_\odot$ star, viewed edge-on from $D = 2.7 \text{ kpc}$. Constant maser absorption coefficient between radii $R_i = 378 \text{ AU}$ ($0''.14$) and $R_o = 1080 \text{ AU}$ ($0''.4$). [See the electronic edition of the *Journal* for a color version of this figure.]

at radius $\rho = r/D$ along a path with displacement θ . The rotation velocity $V(\rho)$ and its LOS component v obey $v/\theta = V/\rho = \Omega$, the angular velocity. In Keplerian rotation $\Omega \propto \rho^{-3/2}$ with $\Omega_o = \Omega(\rho_o) = D(GM/R_o^3)^{1/2}$, where $\rho_o = R_o/D$ is the outer radius and M the central mass. Assume a Gaussian frequency profile for the maser absorption coefficient and denote the radial variation of its magnitude at line center by the normalized profile $\eta(\rho)$ ($\int \eta d\rho = 1$). Then

$$\tau(\theta, v) = \tau_0 \int \eta(\rho) \exp \left\{ -\frac{1}{2} \left[\frac{v - \Omega(\rho)\theta}{\Delta v_D} \right]^2 \right\} \frac{d\rho}{\beta}, \quad (1)$$

where $\beta = [1 - (\theta/\rho)^2]^{1/2}$ and $d\rho/\beta$ is distance along the path. The width Δv_D is taken as constant, although it could vary with ρ because of temperature variation and maser saturation. Saturation typically requires $\tau \geq 10$ – 15 across the disk radius, and the broadening of the absorption profile is then proportional to length in excess of this threshold (Elitzur 1992). If the NGC 7538 IRS 1N disk is located in front of the background source, then the overall amplification with $\tau \sim 18$ implies an optical depth of only 9 across the radius, too low for saturation. If the radio continuum is centered on the star, then the optical depth across the radius is ~ 18 and saturation can be expected to have an effect but only at the very outer segments of the disk, where a decrease in temperature could have an opposite offsetting effect. We will consider these effects in a future publication.

We parameterize η with a power law ρ^{-p} from an inner radius $\rho_i = R_i/D$ to ρ_o . Both τ_0 and Δv_D are set directly from $\tau(0, v)$. Modeling the full $\tau(\theta, v)$ requires two free parameters for the integrand (Ω_o and p) and two for the integration limits (ρ_o and $h = \rho_i/\rho_o$). Figure 2 shows contour plots of $\tau(\theta, v)$ for a representative Keplerian disk around a $30 M_\odot$ protostar with the Δv_D determined from the 12.2 GHz data at $\theta = 0$. The system is viewed edge-on at the adopted distance to NGC 7538.

The lowest contour (3%) outlines the angular velocity $\Omega = v/\theta$ on the disk boundaries. The shallow segments of this contour (lower branch for $\theta < 0$) trace out the disk outer radius. The steeper ones trace the inner radius when $|\theta| < \rho_i$ and the midline when $|\theta| > \rho_i$, where the Keplerian $v \propto |\theta|^{-1/2}$ is evident. Along any path at $|\theta| < \rho_i$, the velocity varies from

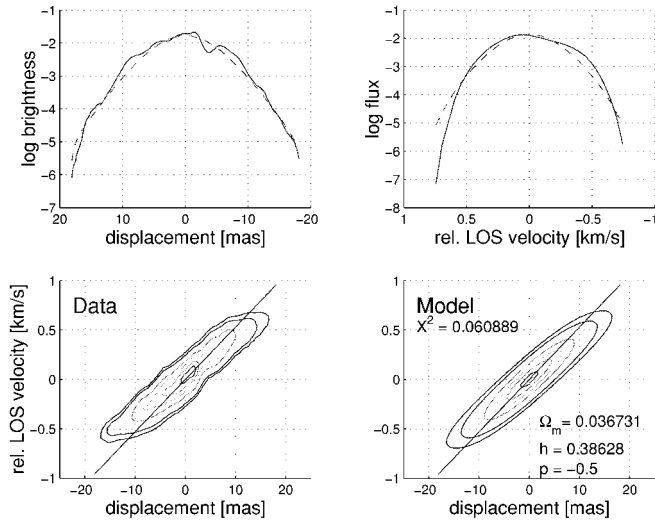


FIG. 3.—Modeling the 12.2 GHz data with a disk with the indicated parameters and $\Delta v_D = 0.4 \text{ km s}^{-1}$. *Top*: θ -variation of frequency-integrated brightness (*left*) and v -variation of the flux (*right*). In both diagrams the log of the quantities is shown. Solid lines show the data, dashed lines the model. *Bottom*: Contour plots of $I(\theta, v)$, the data to the left, the model to the right. The contours of the model have been obtained from the exponential of eq. (1). Contours are 5%, 10%, 30%, 50%, 70%, and 90% of peak. The slope of the diagonal line is Ω_i in units of $\text{km s}^{-1} \text{ mas}^{-1}$. [See the electronic edition of the Journal for a color version of this figure.]

$v_{\min} = \Omega_o |\theta|$ on R_o to $v_{\max} = \Omega_i |\theta|$ on R_i . As long as $v_{\max} - v_{\min} < \Delta v_D$, the full path remains velocity coherent and the maximal τ is centered on the velocity determined from $\partial\tau(v, \theta)/\partial v = 0$. This yields $v = \bar{\Omega}\theta$, where $\bar{\Omega} = \int \Omega \eta d\rho$, an average dominated by the high angular velocity of the inner regions; for example, constant η gives $\bar{\Omega} = 2\Omega_i h / (1 + h^{1/2})$. The linear relation between v and θ is evident in the uniform inclination of the innermost contours.

The condition $v_{\max} - v_{\min} = \Delta v_D$ is met at a displacement θ_k , and τ gets contributions from only a fraction of the path when $\theta > \theta_k$. Since the longest coherence is at the outer radius, where Ω is smallest, the τ -contours bend toward lower velocities, as is evident in Figure 2 around $\theta_k \approx 0''.02$. This bending reflects the change from inner-edge to outer-edge dominance of longest coherence. As θ increases further beyond ρ_i , the longest coherent segment moves from the outer radius to the disk midline. The maximal τ begins to increase, creating the local outer maximum evident in the 50% contours at $\theta \approx 0''.39$ before final truncation at $\theta = \rho_o$.

This discussion shows that the contours of highest amplification, down to 70% of τ_o , contain dependence on p , h , and Ω but not on ρ_o . This has two important consequences: (1) successful modeling of the strongest maser emission requires one less parameter, and (2) since Ω involves only the combination M/R^3 , the central mass cannot be determined without observations of (exponentially weaker) radiation close to the phase-space boundary to determine ρ_o .

Brightness measurements with dynamic range f map the τ -distribution between τ_o and $\tau_o - \ln f$. With $\tau_o = 15.99$ and $f \approx 100$, the 12.2 GHz data trace the τ -contours in NGC 7538 IRS 1N down to 70% of peak. Therefore the data shown in the bottom left map of Figure 3 cover only the two innermost contours in Figure 2, and if our model is applicable it should require only the three parameters h , Ω , and p . In fact, the first two can be determined quite accurately even without detailed modeling since the bend in the τ -contours occurs at $v_k \approx \frac{1}{2} \Delta v_D (1 +$

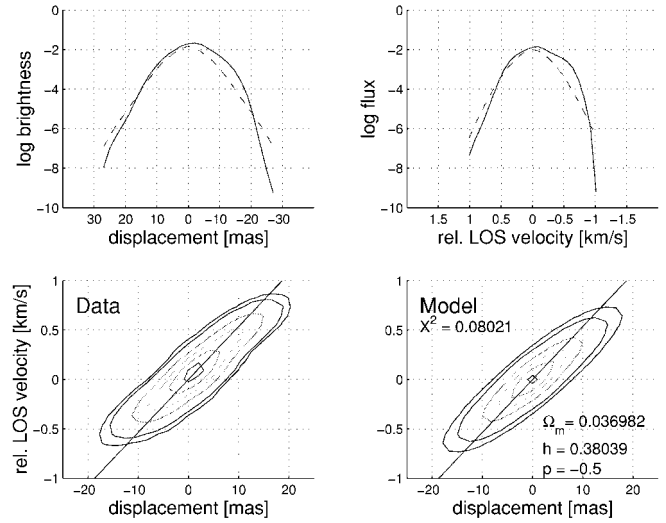


FIG. 4.—Same as Fig. 3 for the 6.7 GHz maser. [See the electronic edition of the Journal for a color version of this figure.]

$h^{3/2}) / (1 - h^{3/2})$ and $\theta_k \approx \Omega_m v_k$, where $\Omega_m = \frac{1}{2}(\Omega_i + \Omega_o)$. We find directly that $h = 0.39$ and $\Omega_m = 0.037 \text{ km s}^{-1} \text{ mas}^{-1}$, implying $M/R^3 = 30 M_\odot / (1000 \text{ AU})^3$ and leaving p as the only free parameter to match all other data points in the (θ, v) -plane. Sensible fits to the 12.2 GHz data are obtained when $0.035 \leq \Omega_m \leq 0.045$ and $0.3 \leq h \leq 0.4$.

The bottom right panel of Figure 3 shows the model map for $p = -0.5$; the top panels show how well the fitting of $\tau(\theta, v)$ reproduces the brightness profile and the spectrum. The negative p means that η , i.e., the maser absorption coefficient, increases with radius. The relation between η and overall density involves the product of the methanol abundance, the fraction of methanol in the maser system, and the fractional inversion. Any of these factors might give more weight to the disk outer regions. Considering the simple power law with sharp cutoffs that we employ, a 70% increase in η across the disk is compatible with a constant density profile.

Our model is equally successful in fitting the main 6.7 GHz maser emission, as is evident from Figure 4. The value of p is the same for this maser; the only slightly different parameters are $\tau_o = 18.32$, $h = 0.38$, and $\Omega_m = 0.037 \text{ km s}^{-1} \text{ mas}^{-1}$. The value for Δv_D was taken from the 12.2 GHz maser, which is considered more reliable because of the higher spatial resolution. Good fits of the 6.7 GHz data are obtained when $0.035 \leq \Omega_m \leq 0.045$ and $0.35 \leq h \leq 0.45$. The virtual identity of the disk segments of such different masing transitions is an important challenge for Class II methanol pumping calculations.

4. DISCUSSION

The analysis presented here shows that a Keplerian disk explains successfully, down to minute details, the main methanol maser feature in NGC 7538 IRS 1N. The angular velocity that we find implies a disk outer radius of $\sim 1000 \text{ AU}$ if the central mass is $30 M_\odot$, as determined by Campbell (1984). The methanol maser emission covers a substantial area of the disk, with the radius varying by a factor of 3.

The $\tau(\theta, v)$ -contours display a bend in the position-velocity diagram. Since $v = \Omega\theta$, a straight line in this diagram implies a constant $\Omega(\rho)$, i.e., either a single radius or, in the case of an extended region, a solid-body rotation. Our analysis therefore uncovers a unique signature of differential rotation in the NGC

7538 IRS 1N disk. The emission's smooth structure and the observation's high sensitivity are crucial for this detection, which is made well inside the $\sim 1.2 \text{ km s}^{-1}$ width of the spectral feature (see top right panels in Figs. 3 and 4). These requirements preclude detection of the effect in extragalactic sources and explain why it could not be considered in the analysis of the H₂O maser disk in NGC 4258 (e.g., Watson & Wallin 1994). However, a bend in the position-velocity diagram has been found in thermal line emission from low-mass stars and interpreted as steep-gradient solid-body rotation inside a shallow-gradient Keplerian outer region (Beckwith & Sargent 1993; Ohashi et al. 1997; Belloche et al. 2002). Since maser and optically thin thermal emission, which is directly proportional to optical depth, share the same kinematic structure, our analysis shows that there is no need to invoke additional components on top of Keplerian rotation.

Our analysis is valid for a radio continuum source placed either behind the maser disk or at its center. The latter possibility would fit well in the context of disk photoevaporation models (Hollenbach et al. 1994). In that case, the radial extent of disk photoevaporation by the central star in NGC 7538 covers the entire maser region and could activate both methanol formation and the observed outflow, responsible for the radio continuum. The maser location at the outflow waistline makes this scenario especially attractive.

The methanol maser data determine detailed disk properties with high precision, yet the central mass remains undetermined since it requires the outer radius. And ρ_o is still unobservable because the angular extent of the detected emission does not trace the full disk; instead it is controlled by velocity coherence and the dynamic range of the observations. The amplification opacity at the disk outer edge (see Fig. 2) is 50% of the central

peak level. With $\tau = 16$ (18) at the center, detection of the outer peak requires a dynamic range of 3000 (8100) if the radio source is located behind the maser disk, placing it beyond the reach of the current observations by a factor of ~ 30 (80). The requirements become even more severe if the continuum is centered on the star. The 6.7 GHz outlier features therefore cannot correspond to the outer peak of our model disk. Instead, these outliers are probably the first detection of enhanced amplification by small inhomogeneities in an otherwise rather smooth disk. Such nonaxisymmetric distortions of the disk surface and their possible effect on the pumping have been proposed by Durisen et al. (2001). It should be possible, though, to determine ρ_o by probing the boundary of the (θ, v) -region at $\theta < \rho_o$ along the v -axis or another direction such as the normal to Ω . We will study these issues in detail in a future publication.

This study provides one of the few pieces of evidence to date for a compact ($\lesssim 1000$ AU) disk around a massive protostar. It seems certain, though, that not all Class II methanol masers occur in disks. Even in NGC 7538 IRS 1N itself, the weaker methanol masers to the south, which are associated with other maser species (OH, H₂O, etc.), are likely to arise from an outflow. The interpretation of ordered lines of methanol masers in terms of disk or outflow models must be decided case by case with detailed modeling.

M. Pestalozzi thanks his fellow Ph.D. student Rodrigo Parra for the useful discussions and for all the useful MATLAB tricks. M. Elitzur thanks the NSF for its support and Chalmers University for a Jubileum Professor award that triggered a most enjoyable visit to Onsala. The reduced 12.2 GHz data cube was kindly made available by Vincent Minier.

REFERENCES

- Akabane, K., Matsuo, H., & Kuno, N. 2001, PASJ, 53, 821
 Beckwith, S., & Sargent, A. 1993, ApJ, 402, 280
 Belloche, A., André, P., Despois, D., & Blinder, S. 2002, A&A, 393, 927
 Campbell, B. 1984, ApJ, 282, L27
 Campbell, B., & Thompson, R. 1984, ApJ, 279, 650
 Cesaroni, R., et al. 1999, A&A, 345, 949
 DeBuizer, J. 2003, MNRAS, 341, 277
 Durisen, R. H., Mejia, A. C., Pickett, B. K., & Hartquist, T. W. 2001, ApJ, 563, L157
 Elitzur, M. 1992, ARA&A, 30, 75
 Fuente, A., Rodríguez-Franco, A., Testi, L., Natta, A., Bachiller, R., & Neri, R. 2003, ApJ, 598, L39
 Gaume, R., Goss, W., Dickel, H., Wilson, T., & Johnston, K. 1995, ApJ, 438, 776
 Hollenbach, D., Johnstone, D., Lizano, S., & Shu, F. 1994, ApJ, 428, 654
 Minier, V., Booth, R., & Conway, J. 1998, A&A, 336, L5
 ———. 2000, A&A, 362, 1093
 Minier, V., Conway, J., & Booth, R. 2001, A&A, 369, 278
 Molinari, S., Brand, J., Cesaroni, R., & Palla, F. 2000, A&A, 355, 617
 Momose, M., et al. 2001, ApJ, 555, 855
 Moscadelli, L., Menten, K., Walmsley, C., & Reid, M. 2002, ApJ, 564, 813
 Norris, R., et al. 1998, ApJ, 508, 275
 Ohashi, N., Hayashi, M., Ho, P., & Momose, M. 1997, ApJ, 475, 211
 Qi, C., Kessler, J. E., Koerner, D. W., Sargent, A. I., & Blake, G. A. 2003, ApJ, 597, 986
 Sandel, G., Wright, M., & Forster, J. 2003, ApJ, 590, L45
 Shepherd, D., Claussen, M., & Kurtz, S. 2001, Science, 292, 1513
 Watson, W., & Wallin, B. 1994, ApJ, 432, L35
 Willner, S. 1976, ApJ, 206, 728

ERRATUM: “A CIRCUMSTELLAR DISK IN A HIGH-MASS STAR-FORMING REGION” (ApJ, 603, L113 [2003])

MICHELE R. PESTALOZZI, MOSHE ELITZUR, JOHN E. CONWAY, AND ROY S. BOOTH

For a central mass of $30 M_{\odot}$, the outer radius of the maser disk is $R_0 \sim 750$ AU instead of the 1000 AU listed in the above-mentioned Letter. The inner radius is $R_i \sim 290$ AU instead of the 350 AU listed. In the Figures 3 and 4, the angular velocity Ω_m should be listed as $0.055 \text{ km s}^{-1} \text{ mas}^{-1}$ instead of $0.037 \text{ km s}^{-1} \text{ mas}^{-1}$. The slope of the diagonal line in the bottom panels of each figure is Ω_m rather than Ω_i . We thank A. Jerkstrand for spotting these mistakes and an error in the modeling computer program.